Supporting Information

[28]Hexaphyrin derivatives for anion recognition in organic and aqueous media

Flávio Figueira,[a] Andreia S. F. Farinha,[a] Paulino V. Muteto,[b] Marcelo D. Polêto,[c] Hugo Verli,[c] M. Teresa S. R. Gomes,[b] Augusto C. Tomé,[a] José A. S. Cavaleiro[a] and João P. C. Tomé*[a,d]

[a]*QOPNA,* [b]*CESAM and Department of Chemistry, University of Aveiro, 3810-193 Aveiro, Portugal*

[c]*Center of Biotechnology, Federal University of Rio Grande do Sul, Brazil*

[d]*Department of Organic and Macromolecular Chemistry, Ghent University, B-9000 Gent, Belgium*

Contents

1 Experimental Section

1.1 General information

^{1}H, ^{13}C, and ^{19}F solution NMR spectra were recorded on a *Bruker Avance-300* spectrometer at 300.13, 75.47 and 282.38 MHz, respectively. Tetramethylsilane was used as internal reference. HRMS spectra were recorded on VG *AutoSpec-M* spectrometer; using chloroform and methanol as solvent, with 3-nitrobenzyl alcohol (NBA) as matrix. Absorption spectra were recorded in chloroform using a *Shimadzu UV-2501-PC*. Analytical TLC was carried out on precoated silica gel sheets (Merck, 60, 0.2 mm). Column chromatography was carried out over silica gel (Merck, 230–400 mesh).

1.2 Synthesis

***meso*-Hexakis(pentafluorophenyl)[26]hexaphyrin, (1):** This compound was prepared following a reported procedure.[1]

^{1}H NMR (300 MHz, $CDCl_3$): δ 7.74 (d, *J* = 4.7 Hz, 4H, β-H), 7.64 (d, *J* = 4.7 Hz, 4H, β-H), 4.39 (s, 2H, NH), 2.54 (s, 4H, β-H). **^{13}C NMR** (75 MHz, $CDCl_3$): δ 149.99, 147.92 – 147.45 (m), 147.07 – 146.45 (m), 145.47, 144.65 – 144.20 (m), 143.53 (d, *J* = 3.6 Hz), 140.45 – 139.04 (m), 136.54 – 135.72 (m), 135.28, 130.24, 129.21, 119.41, 113.27 – 112.05 (m), 100.08, 96.19, 30.30. **^{19}F NMR** (282 MHz, $CDCl_3$): δ -160.91 (dd, *J* = 24.2, 7.2 Hz, 4F, *o*-F), -161.18 (d, *J* = 15.4 Hz, 8F, *o*-F), -174.38 (t, *J* = 20.9 Hz, 2F, *p*-F), -176.08 (t, *J* = 20.8 Hz, 4F, *p*-F), -183.35 – -183.85 (m, 4F, *m*-F), -184.46 – -185.01 (m, 8F, *m*-F).

General procedure for compounds 2 and 3: To a solution of **1** (100.0 mg, 0.068 mmol) in NMP (5 mL), were added *N*-tosylethylenediamine (30 equiv.) or *N*-isopropylethylenediamine (30 equiv.) and triethylamine (2 mL). The mixture was heated at 105 ºC for 24 h and then the reaction mixture was cooled to r.t., quenched with a mixture of CH_2Cl_2/MeOH (5%) and washed successively with a saturated solution of citric acid (50 mL) and H_2O (3 x 100 mL). The organic phase was dried over Na_2SO_4 and concentrated. The residue was chromatographed on silica gel using CH_2Cl_2/MeOH (4%) (for **2**) or CH_2Cl_2/MeOH/NEt_3 (7:2.8:0.2) (for **3**) as eluents. The blue bands were collected and crystallized from CH_2Cl_2/MeOH to yield **2** (120 mg, 69%) or **3** (85 mg, 64%) as blue solids.

***meso*-Hexakis[2,3,5,6-tetrafluoro-4-(*N*'-tosylethylenediamino)phenyl][28]hexaphyrin, (2):**

^{1}H NMR (300 MHz, DMSO-d_6): δ 7.94 – 7.59 (m, 26 H, 4 NHTs, 8 β-H and 12 ArTs), 7.43 (d, *J* = 8.1 Hz, 4H, ArTs), 7.34 (d, *J* = 8.1 Hz, 8H, ArTs), 6.23 (s, 2H, ArN**H**CH_2), 6.11 (s, 4H,

ArN**H**CH_2), 4.52 (s, 4H, NH Inner), 3.62 – 3.47 (m, 4H, ArNHC**H**$_2$), 3.50 (signal overlapped in water, see Figure SI 29, 8H, ArNHC**H**$_2$) 3.12-3.05 (m, 4H, C**H**$_2$NHTs), 2.95-2.89 (m, 8H, C**H**$_2$NHTs), 2.36 (s, 6H, CH_3), 2.28 (s, 12 H, CH_3). **^{13}C NMR** (75 MHz, DMSO-d_6) δ 149.70 (s), 148.49 – 146.71 (m), 145.50 – 143.28 (m), 142.73, 138.06 (ddd, J = 48.7, 27.3, 10.6 Hz), 134.96 (dd, J = 30.3, 17.9 Hz), 132.22 – 129.18 (m), 129.68, 128.35 (d, J = 12.7 Hz), 126.55, 117.18, 104.61, 96.23, 45.68 – 44.91 (m), 44.91 – 43.27 (m), 44.47 – 41.04 (m), 20.99 (d, J = 7.9 Hz). **^{19}F NMR** (282 MHz, DMSO-d_6) δ -166.13 (d, J = 19.9 Hz, 4F, *o*-F), -166.94 (s, 8F, *o*-F), -183.45 (d, J = 19.7 Hz, 4F, *m*-F), -184.42 (d, J = 19.5 Hz, 8F, *m*-F).

^{1}H NMR (300 MHz, $CDCl_3$): δ 7.89 – 7.78 (m, 8H, β-H), 7.74 (d, J = 8.2Hz, 4H, ArTs), 7.70 (d, J = 8.2 Hz, 8H, ArTs), 7.34 (d, J = 8.2 Hz, 4H, ArTs), 7.18 (d, J = 8.2 Hz, 8H, ArTs), 6.81 (t, J = 5.7 Hz, 2H, NHTs), 6.66 (t, J = 5.7 Hz, 4H, NHTs), 4.98 (s, 2H, ArN**H**CH_2), 4.87 (s, 4H, ArN**H**CH_2), 3.82-3.66 (m, 4H, ArNHC**H**$_2$), 3.50-3.45 (m, 8H, ArNHC**H**$_2$), 3.28-3.23 (m, 4H, C**H**$_2$NHTs), 3.12-3.10 (m, 8H, C**H**$_2$NHTs), 2.63 – 2.51 (m, 4H, β-H), 2.39 (s, 6H, CH_3), 2.22 (s, 12H, CH_3).

HRMS-ESI found: 2627.5335 ([M+H]$^+$); calculated for $C_{120}H_{95}F_{24}N_{18}O_{12}S_6$ (2627.5312).

***meso*-Hexakis[2,3,5,6-tetrafluoro-4-(*N*'-isopropylethylenediamino)phenyl][28]hexaphyrin, (3):**

^{1}H NMR (300 MHz, DMSO-d_6): δ 7.71 (d, J = 8.4 Hz, 8H, β-H), 6.14 (s, 2H, ArN**H**CH_2), 6.04 (s, 4H, ArN**H**CH_2), 3.37 (signals overlapped in water, see Figure SI 34, 2 and 4 H, ArNHC**H**$_2$) 2.91-2.84 (m, 2H, -C**H**$_2$NHC$(CH_3)_2$), 2.76 – 2.73 (m, 4H, -C**H**$_2$NHC$(CH_3)_2$), 1.27-1.18 (m, 4H, β-H), 1.06 (d, J = 6.2 Hz, 12H, -C(C**H**$_3)_2$), 0.98 (d, J = 6.2 Hz, 24H, -C(C**H**$_3)_2$). **^{13}C NMR** (75 MHz, DMSO-d_6): δ 178.34, 148.24 – 145.38 (m), 145.83 – 142.56 (m), 138.98 – 136.23 (m), 135.09 (dd, J = 32.5, 13.6 Hz), 130.24 – 127.08 (m), 117.35, 103.78 (dd, J = 69.8, 61.2 Hz), 63.05 – 61.75 (m), 52.01, 48.03 (d, J = 5.7 Hz), 46.64, 44.71, 22.56. **^{19}F NMR** (282 MHz, DMSO-d_6): δ -166.19 (d, J = 19.7 Hz, 4F, *o*-F), -166.94 (s, 8F, *o*-F), -183.73 (d, J = 21.5 Hz, 4F, *m*-F), -184.72 (d, J = 20.3 Hz, 4F, *m*-F).

HRMS-ESI found: 1955.7584 ([M+H]$^+$); calculated for $C_{96}H_{95}F_{24}N_{18}$ (1955.7598).

2 Anion binding interaction in organic medium

2.1 UV-Vis spectroscopic titration of chemosensors 1-3 with anions in $CHCl_3$ and DMSO

The anion binding tests in $CHCl_3$ and DMSO were carried out at 22 °C and were followed by UV-Vis spectroscopy. Several anions, such as fluoride, chloride, bromide, acetate, dihydrogen

phosphate, nitrate and nitrite (all in the form of tetrabutylammonium salts), were used. Equations (1) and (2) were used for the determination of the affinity constants.[2]

Non-linear regression for the 1:1 (hexaphyrin: anion) complex (K units are M^{-1})

$$\frac{A}{l} = \frac{[sensor].K.\Delta\epsilon.[Anion]}{1 + K.[Anion]} \quad (1)$$

Non-linear regression for the 1:2 (hexaphyrin: anion) complex (K units are M^{-2})

$$\frac{A}{l} = \frac{[sensor].K11.\Delta\epsilon11.[Anion] + K11.K12\ .\Delta\epsilon12.[Anion]2}{1 + K.[Anion] + K11.K12.[Anion]2} \quad (2)$$

Where A is the absorbance, l the path length, K the affinity constant, Δε is the molar absorptivity coefficient, [sensor] and [anion] are the concentrations of the sensor and anion, respectively.

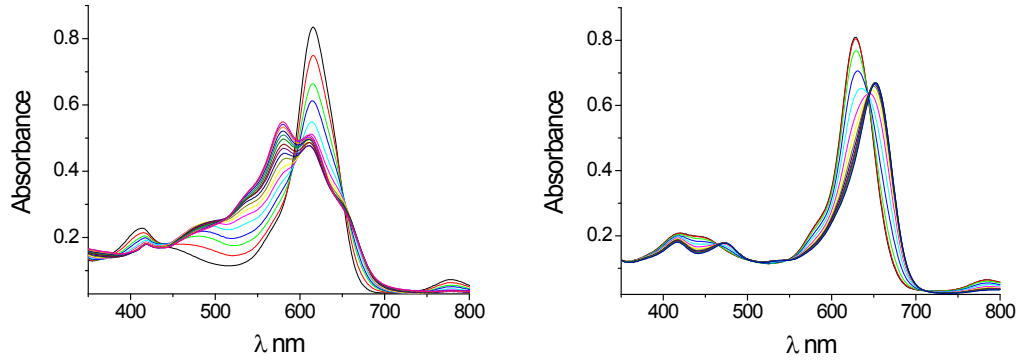

Figure SI 1: Titration examples of **1** with: **left)** fluoride anion in $CHCl_3$; **right)** fluoride anion in DMSO.

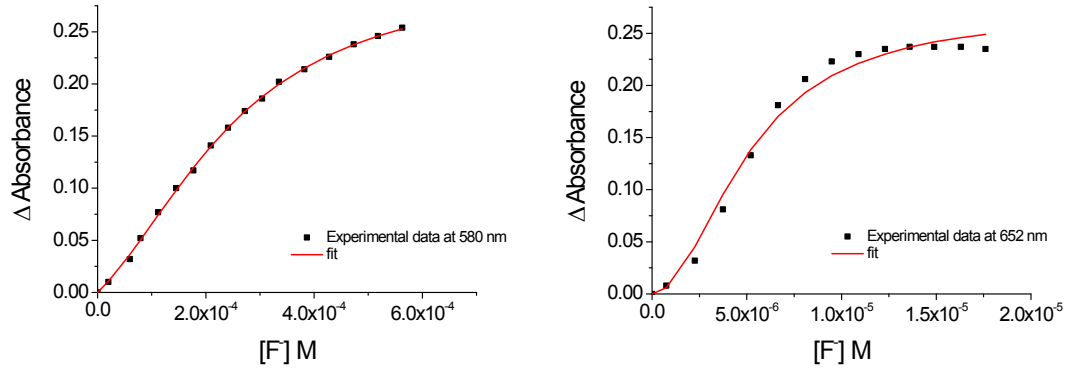

Figure SI 2: Experimental data and fit titration at of compound **1** with: **left**) fluoride anion in $CHCl_3$; **right)** fluoride anion in DMSO.

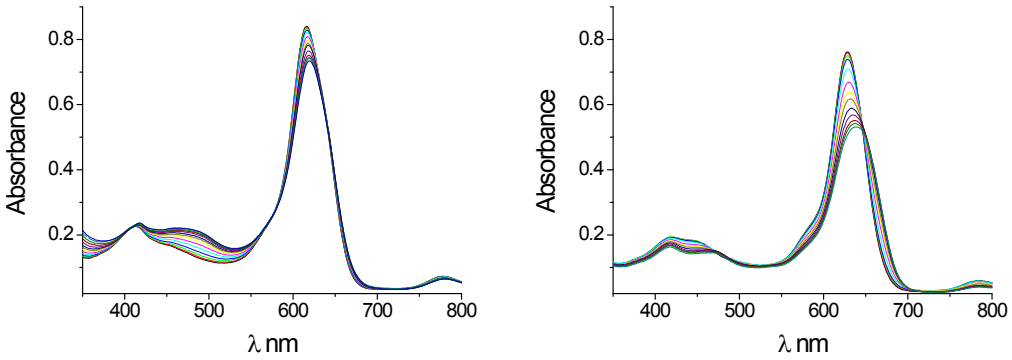

Figure SI 3: Titration examples of **1** with: **left)** acetate anion in $CHCl_3$; **right)** acetate anion in DMSO.

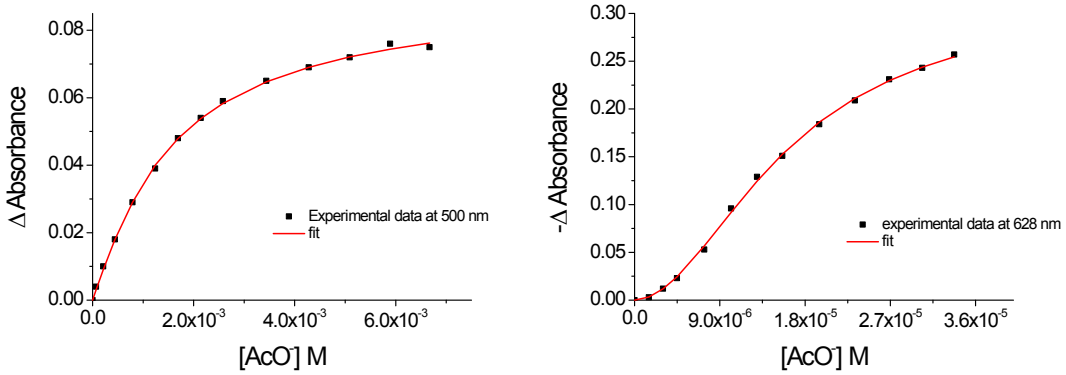

Figure SI 4: Experimental data and fit titration at of compound **1** with: **left**) acetate anion in $CHCl_3$; **right)** acetate anion in DMSO.

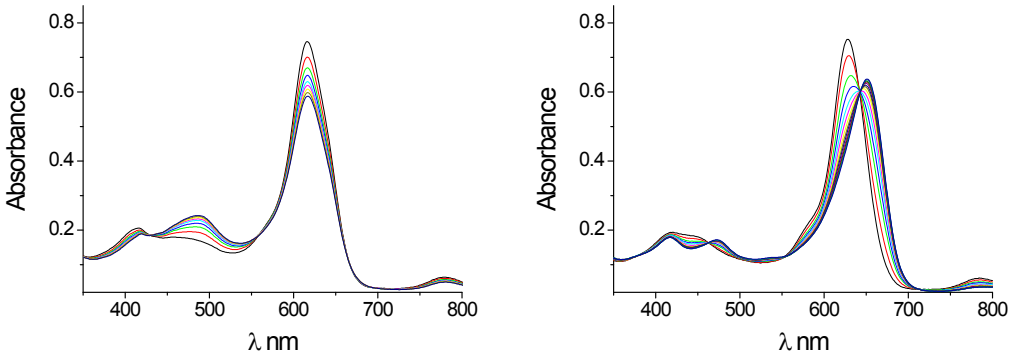

Figure SI 5: Titration examples of **1** with: **left)** dihydrogen phosphate anion in $CHCl_3$; **right)** dihydrogen phosphate in DMSO.

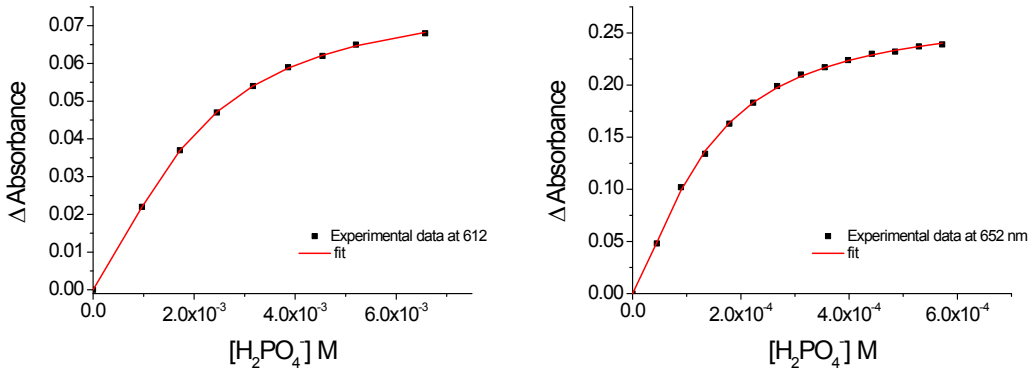

Figure SI 6: Experimental data and fit titration at of compound **1** with: **left)** dihydrogen phosphate anion in $CHCl_3$; **right)** dihydrogen phosphate anion in DMSO.

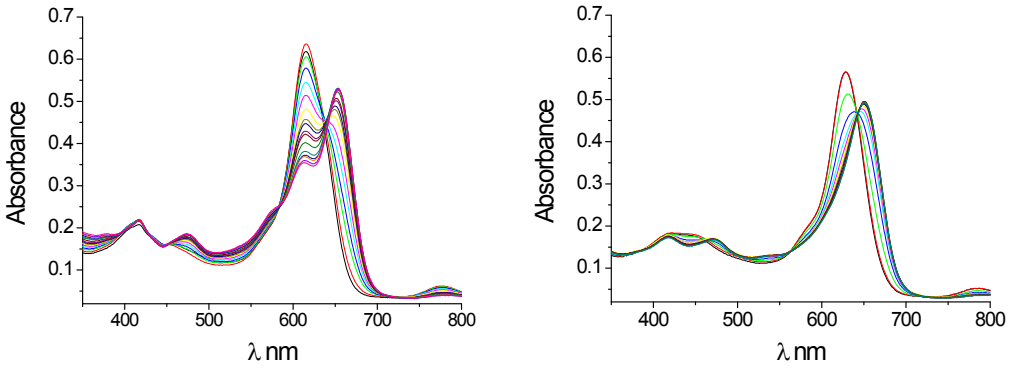

Figure SI 7: Titration examples of **2** with: **left)** fluoride anion in $CHCl_3$; **right)** fluoride anion in DMSO.

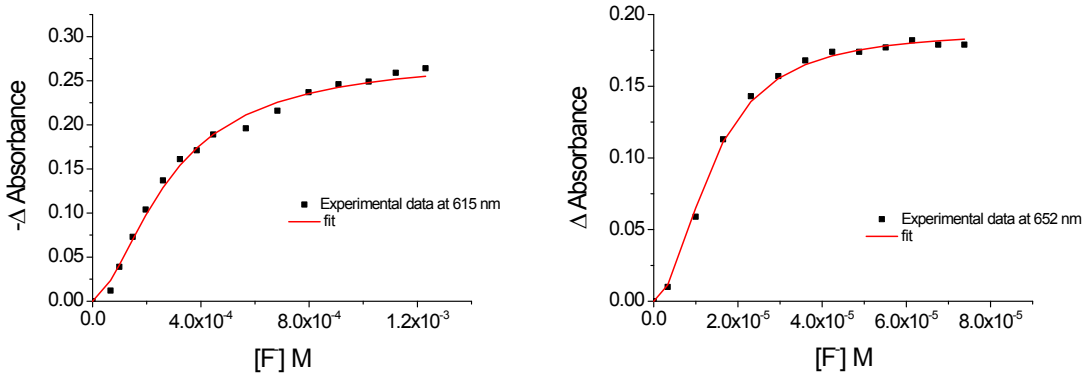

Figure SI 8: Experimental data and fit titration at of compound **2** with: **left**) fluoride anion in $CHCl_3$; **right)** fluoride anion in DMSO.

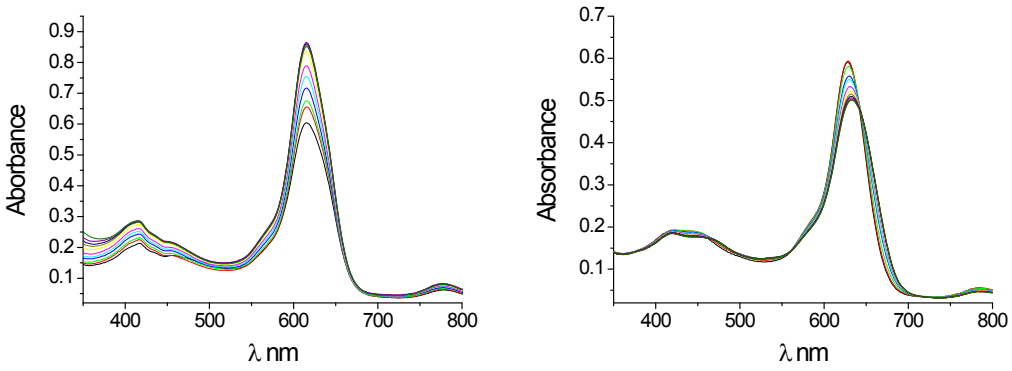

Figure SI 9: Titration examples of **2** with: **left)** acetate anion in $CHCl_3$; **right)** acetate anion in DMSO.

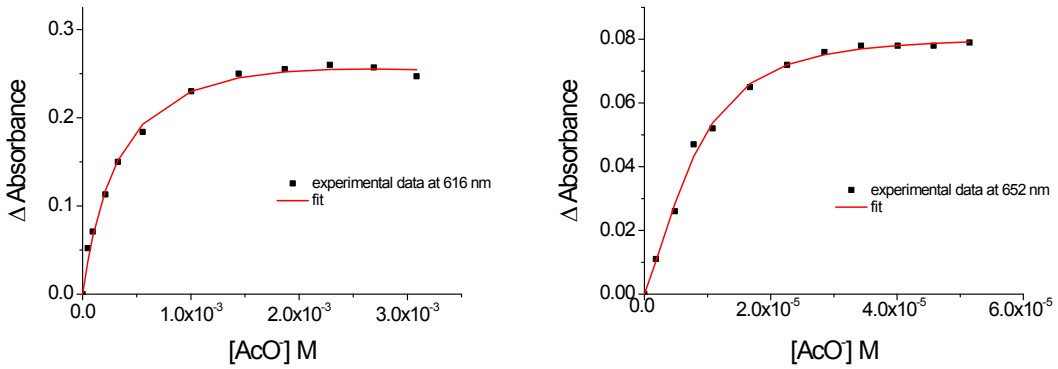

Figure SI 10: Experimental data and fit titration at of compound **2** with: **left**) acetate anion in $CHCl_3$; **right)** acetate anion in DMSO.

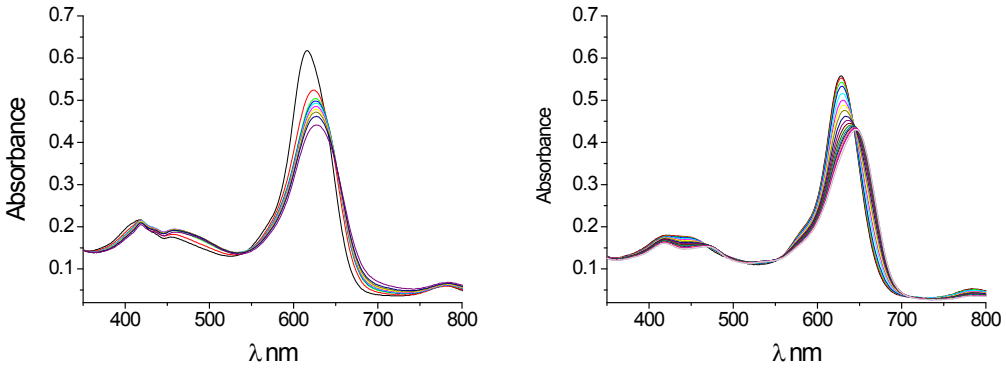

Figure SI 11: Titration examples of **2** with: **left)** dihydrogen phosphate anion in $CHCl_3$; **right)** dihydrogen phosphate in DMSO.

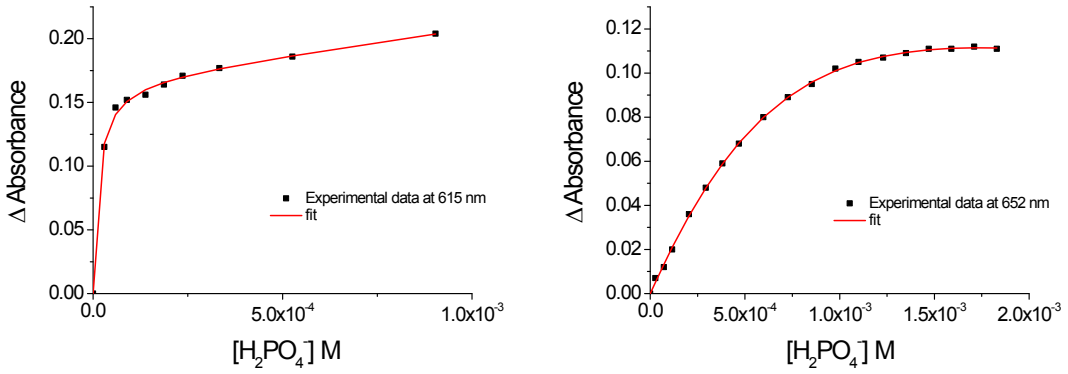

Figure SI 12: Experimental data and fit titration at of compound **2** with: **left)** dihydrogen phosphate anion in $CHCl_3$; **right)** dihydrogen phosphate anion in DMSO.

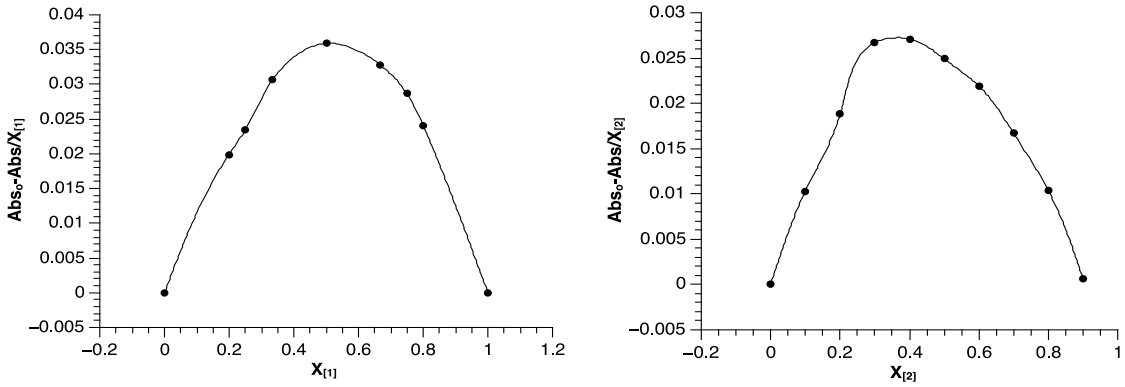

Figure SI 13: Job plot for compounds **1** (left) and **2** (right) with Fluoride anion in DMSO. The total concentration used for compounds **1** and **2** was $1x10^{-6}$ and the plots were achieved from variations in absorption at 630 and 650 nm, respectively.

2.2 ^{1}H NMR spectroscopic titration studies involving the neutral or protonated forms of hexaphyrins 1-3

The anion binding studies were carried out in $CDCl_3$ and DMSO-d_6 and using ^{1}H NMR spectroscopy. The titrations were performed using solutions (around 1 mM) of each hexaphyrin and then adding between 0.1 to 2.5 equivalents of the TBA salts of various test anions. The variation of the signals corresponding to the NH protons was used to infer the main interactions established between the hexaphyrin and the anion (e.g., hydrogen bonding vs. deprotonation).

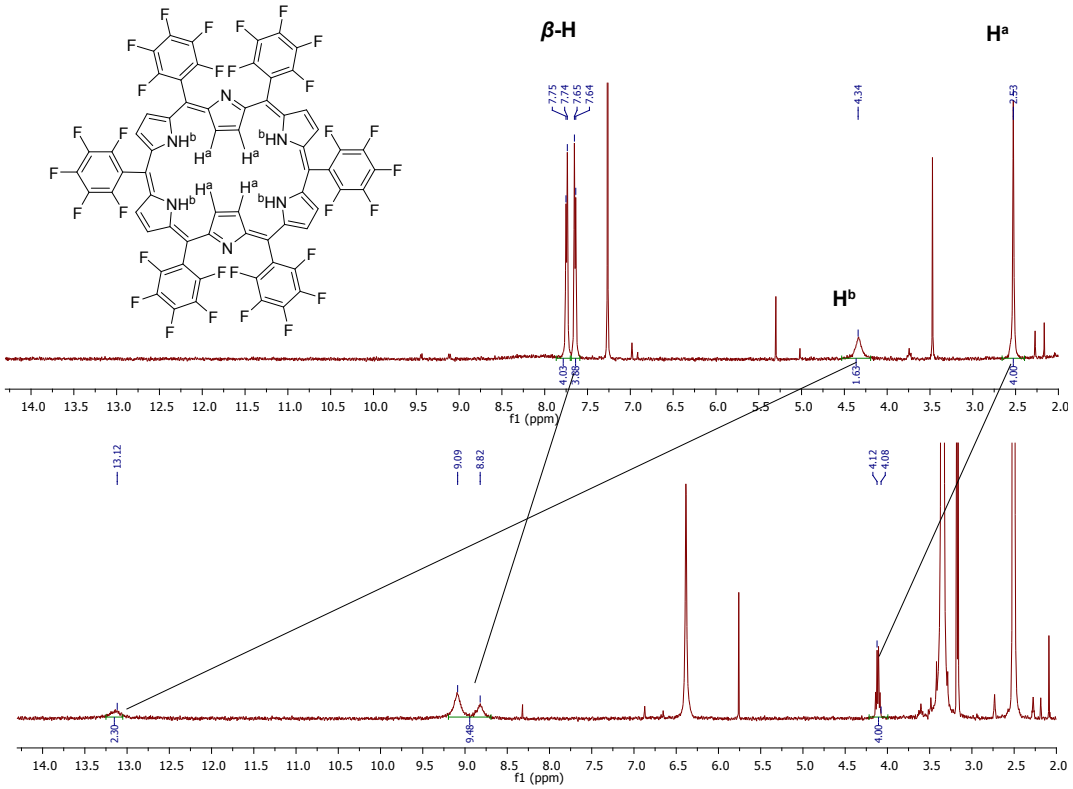

Figure SI 14: ^{1}H NMR spectra of **1** in $CDCl_3$ (up) and DMSO-d_6 (down).

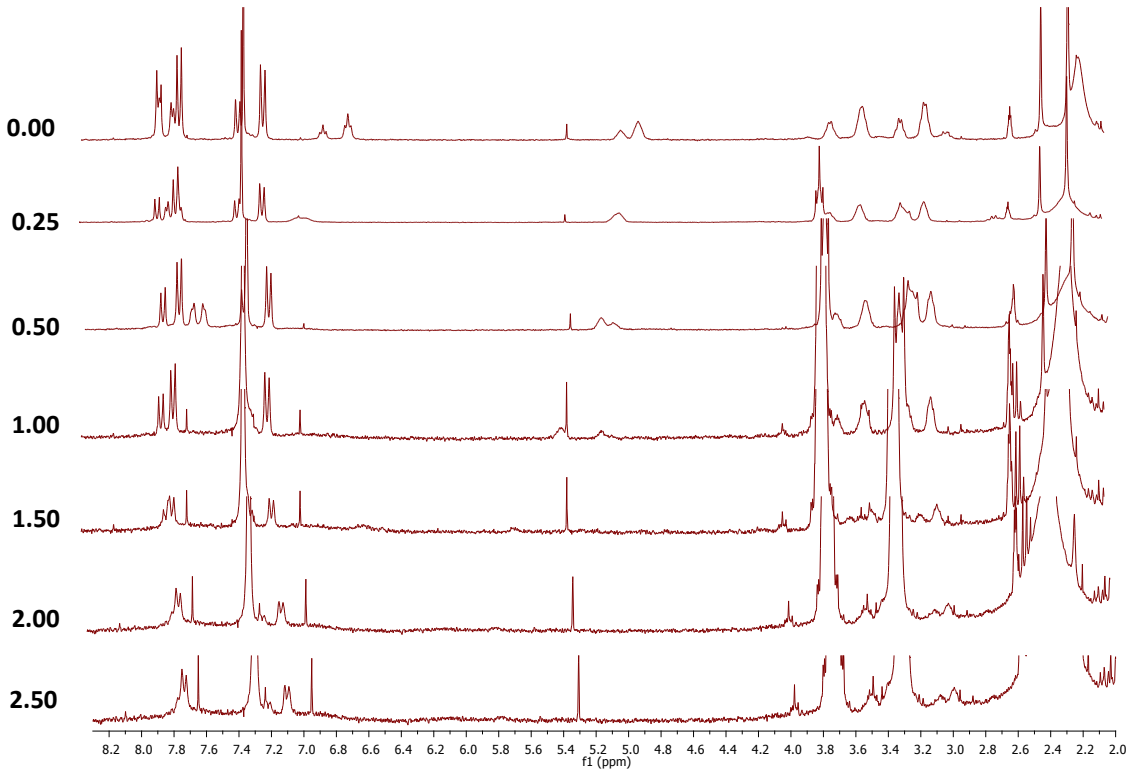

Figure SI 15: ^{1}H NMR spectra of compound **2** in $CDCl_3$ upon addition of fluoride.

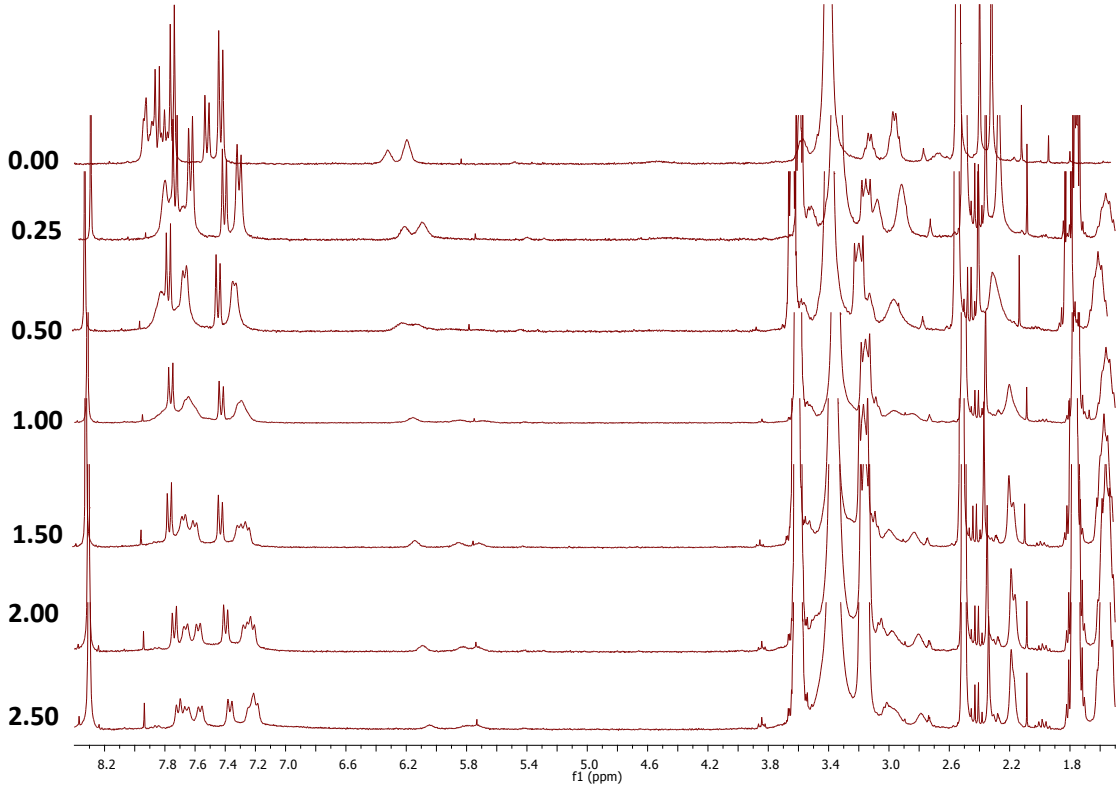

Figure SI 16: ^{1}H NMR spectra of compound **2** in DMSO upon addition of fluoride.

2.3 Molecular dynamic simulations methods:

Once all chemical compounds were properly parameterized, a cubic box was built around hexaphyrin molecules with a distance of 9 nm from its center. Following the 2:1 proportion used in experimental procedures, two molecules of anion were randomly inserted, so as tetrabutylammonium, to guarantee a proper neutral environment. Next, the boxes were filled with $CHCl_3$ or DMSO. The systems were then carefully minimized and restraint forces were applied to solute in a NVT ensemble, followed by a NPT ensemble in order to guarantee a proper termodynamical behavior. The systems were simulated through 10 ns in the absence of restraints, allowing interactions between ions and hexaphyrin to be calculated throughout time. For all simulations, integration step of 2fs and LINCS algorithm was used along a cut-off radius of 1nm for all non-bonded interactions. Each system was simulated in triplicates using random position for ions insertion.

2.3.1 Binding modes of 3 and AcO^- in DMSO:

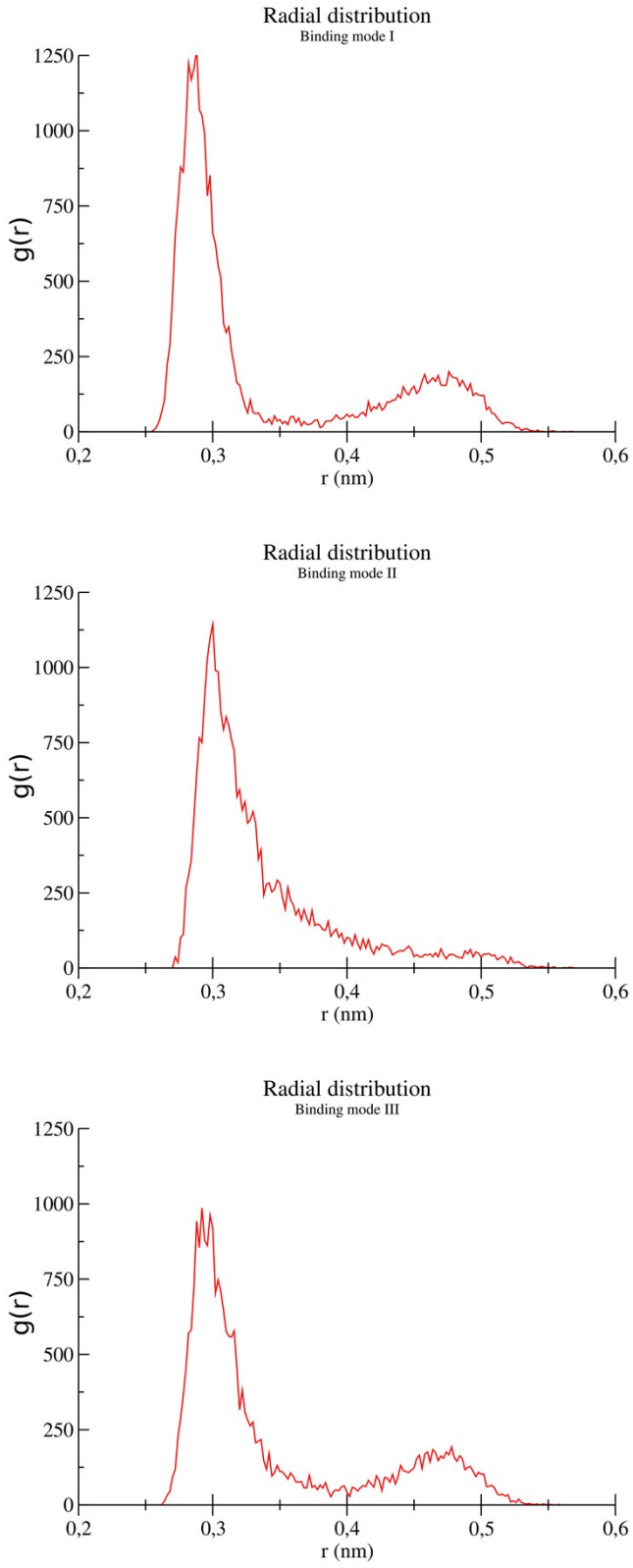

Figure SI 17: Binding mode I (upper), binding mode II (middle) and binding mode III (lower). Each binding mode was obtained from independent simulations and combined for a single illustration. Radial distribution function was calculated between hexaphyrin **3** N atoms and acetate oxygen atoms.

2.4 Colorimetric response

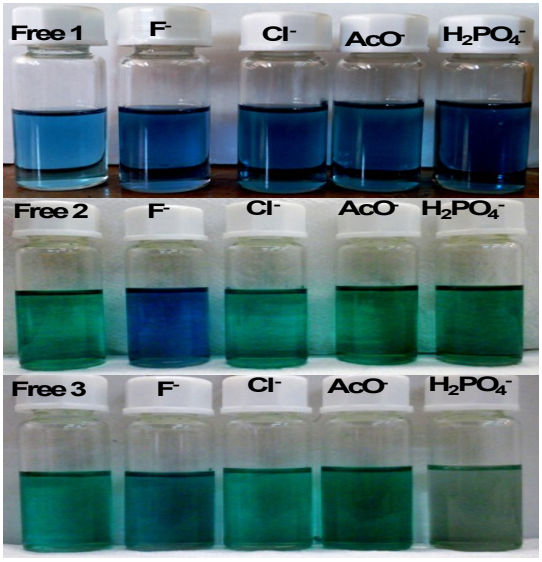

Figure SI 18: Changes in the color of DMSO solutions of hexaphyrins 1-3 (≈ 5.7 μM) upon addition of different anion solutions, as tetrabutylammonium salts (60 μM).

3 Anion-receptor interactions in aqueous medium

Apparatus: piezoelectric quartz crystals were 9 MHz AT-cut HC-6/U with gold electrodes deposited over a chromium layer (ICM-International Crystal Manufacturing Co, Inc). A spin coater (Süss Delta 10 BM) was used to coat the quartz crystals with a chloroform or tetrahydrofuran solution of the selected hexaphyrin. The quartz crystal was inserted on a Teflon cell coupled to a glass cup able to hold 10 mL of the liquid sample. The glass cell had an external jacket through which circulated water at the desired temperature. Figure SI16 shows the experimental layout used in the adsorption experiments. The crystal was connected to an oscillator (ICM-International Crystal Manufacturing Co, Inc) and the frequency was recorded on a PC connected by GPIB to a frequency counter (Leader LF827).

Procedure: After coating, the quartz crystal was left for two days drying at room temperature. The coating amount is related to the observed frequency decrease due to coating ($F_{coating}$). The coated quartz crystal was inserted in the Teflon cell (coated face up), and 10,00 mL of distilled water were added to the glass cup. The water circulating on the external jacket of the cell was at 22 ºC. The frequency of the quartz crystal was recorded. Successive additions of precisely measured volumes of the desired anion standard solution were added in sequence to the water. For each addition, frequency was recorded after stabilization, and the difference between

this reading and the initial frequency, recorded when the crystal was in contact with distilled water, was computed (Δf).

Langmuir model, for the case of adsorption processes can be translated by the following expression:

$$\frac{1}{[Anion]_{ad}} = \frac{1}{K[Anion]_{\infty}} \times \frac{1}{[Anion]_{eq}} + \frac{1}{[Anion]_{\infty}}$$

Where $[Anion]_{ad}$ is the molar adsorption density of the Anion of molecular mass M_{Anion} on the coating, with molecular mass $M_{coating}$, $[Anion]_{\infty}$ is adsorbed anion at saturation, and $[Anion]_{eq}$ is the equilibrium concentration of the anion in solution.

The piezoelectric sensor allows us to obtain Δf , the observed frequency decrease on the coated crystal at equilibrium, and $\Delta f_{coating}$, which is the frequency decrease due to coating, which are proportional to the mass of the ion adsorbed on the surface of the quartz crystal, and to the amount of the hexaphyrin that coated the piezoelectric quartz crystal, respectively.

By plotting $\frac{\Delta f_{coating} \times M_{Anion}}{\Delta f \times M_{coating}}$ *vs* $\frac{1}{[Anion]_{eq}}$ the value of K can be found.

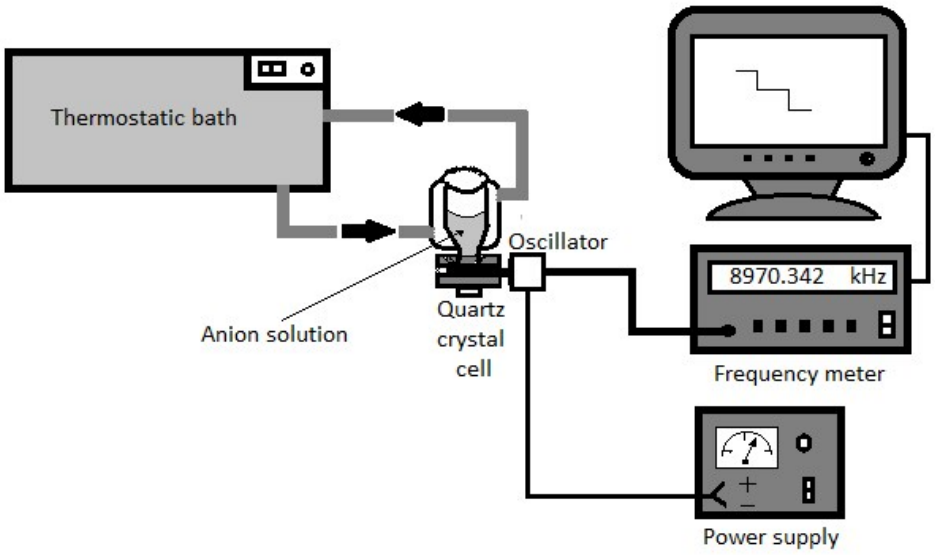

Figure SI 19: Experimental layout containing a piezoelectric quartz crystal coated with hexaphyrins **1**, **2** or **3**.

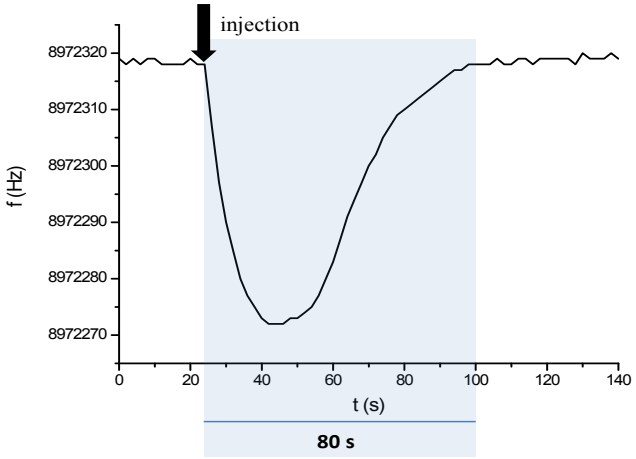

Figure SI 20: Frequency shift seen for a piezoelectric sensor made with **2**, before and after exposition to 0.5 mL of a 5.0×10^{-5} mol L^{-1} aqueous fluoride solution

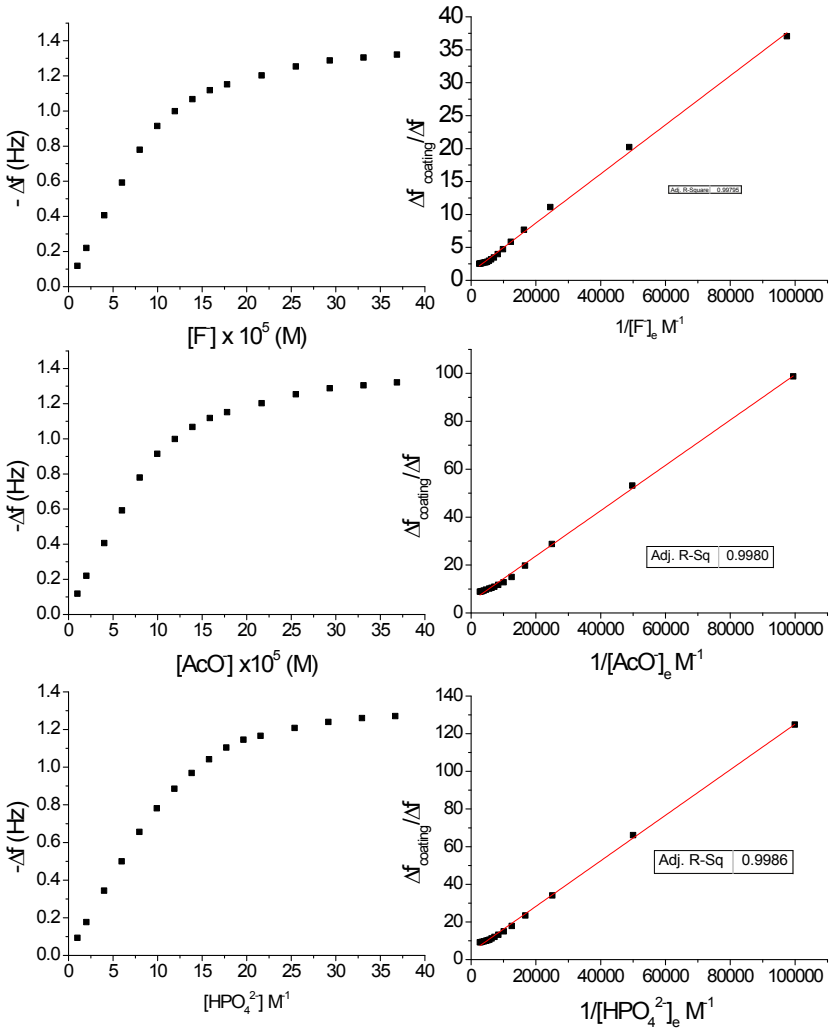

Figure SI 21: Adsorption isotherm (T=22.0 °C) for compound **1** deposited onto the electrode of the piezoelectric quartz crystal, which was in contact with an aqueous solution of the corresponding anion.

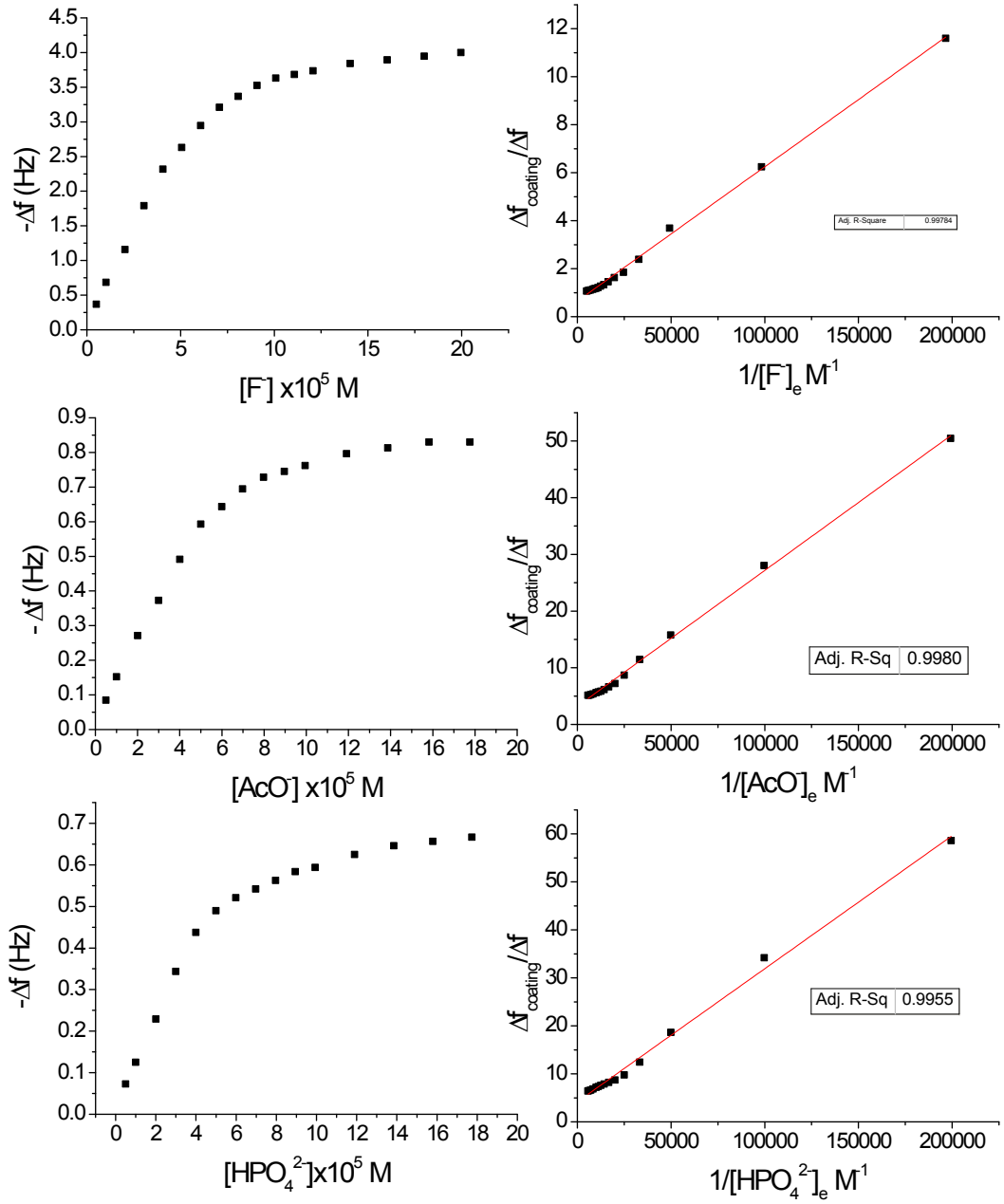

Figure SI 22: Adsorption isotherm (T=22.0 °C) for compound **2** deposited onto the electrode of the piezoelectric quartz crystal, which was in contact with an aqueous solution of the corresponding anion.

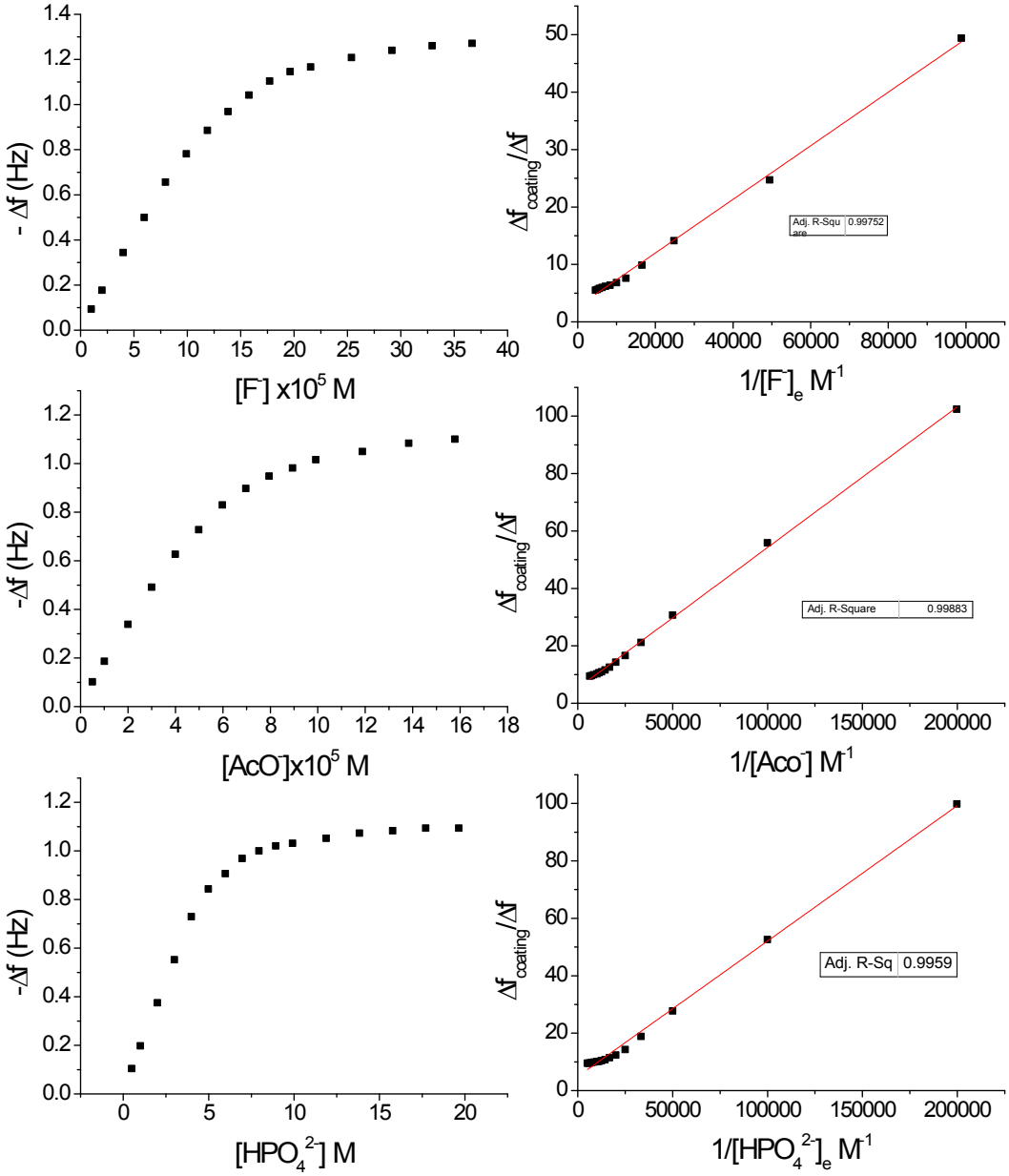

Figure SI 23: Adsorption isotherm (T = 22.0 °C) of compound **3** deposited onto the electrode of the piezoelectric quartz crystal, which was in contact with an aqueous solution of the corresponding anion.

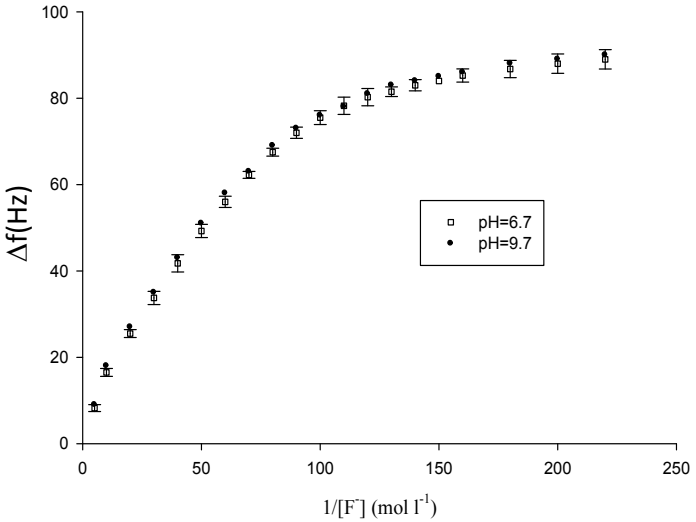

Figure SI 24: Adsorption isotherm (T = 22.0 °C) of compound **2** deposited onto the electrode of the piezoelectric quartz crystal, which was in contact with an aqueous solution of sodium fluoride, at pH 6.7 and 9.7.

4 NMR spectra and mass spectrometric data for all compounds

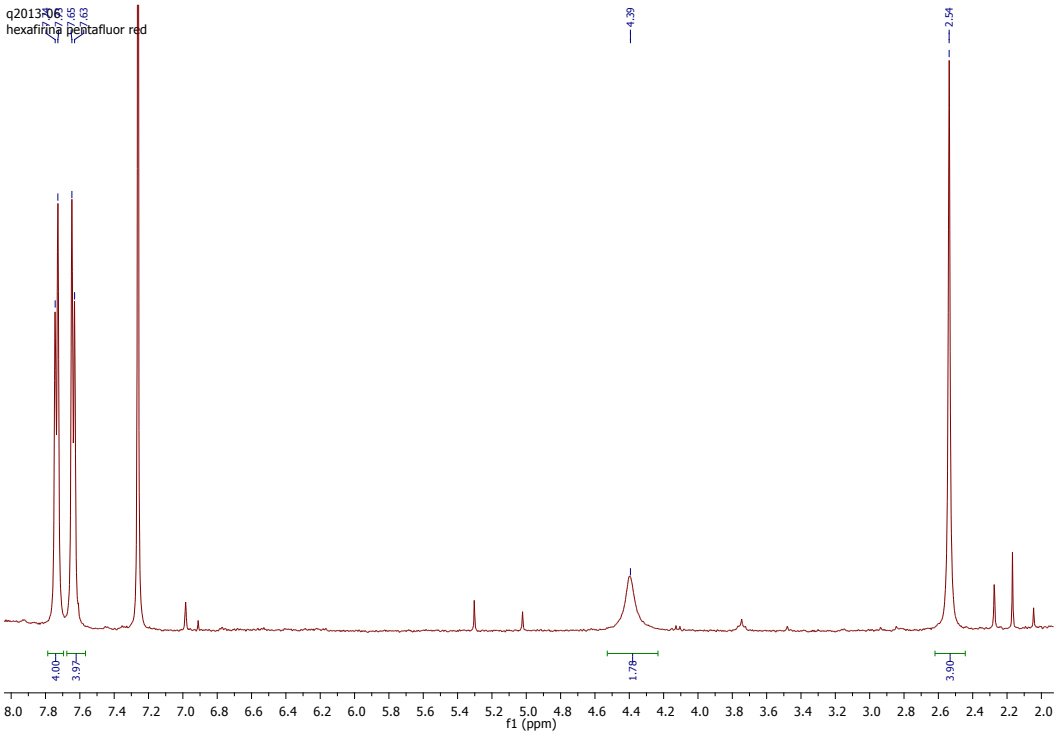

Figure SI 25: ^{1}H NMR spectrum of compound **1** in $CDCl_3$

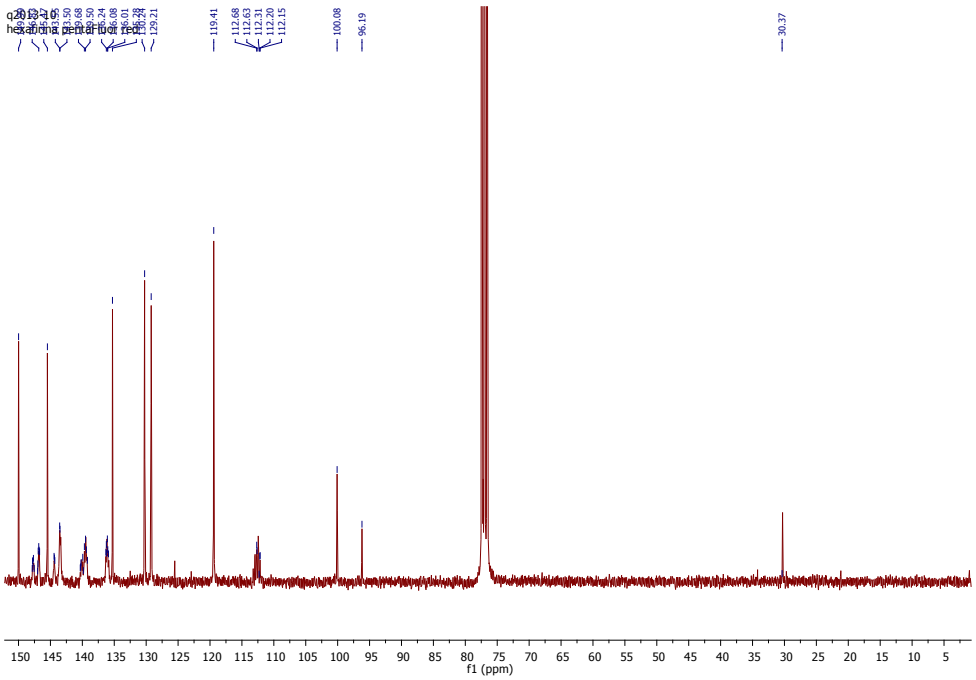

Figure SI 26: ^{13}C NMR spectrum of compound **1** in $CDCl_3$

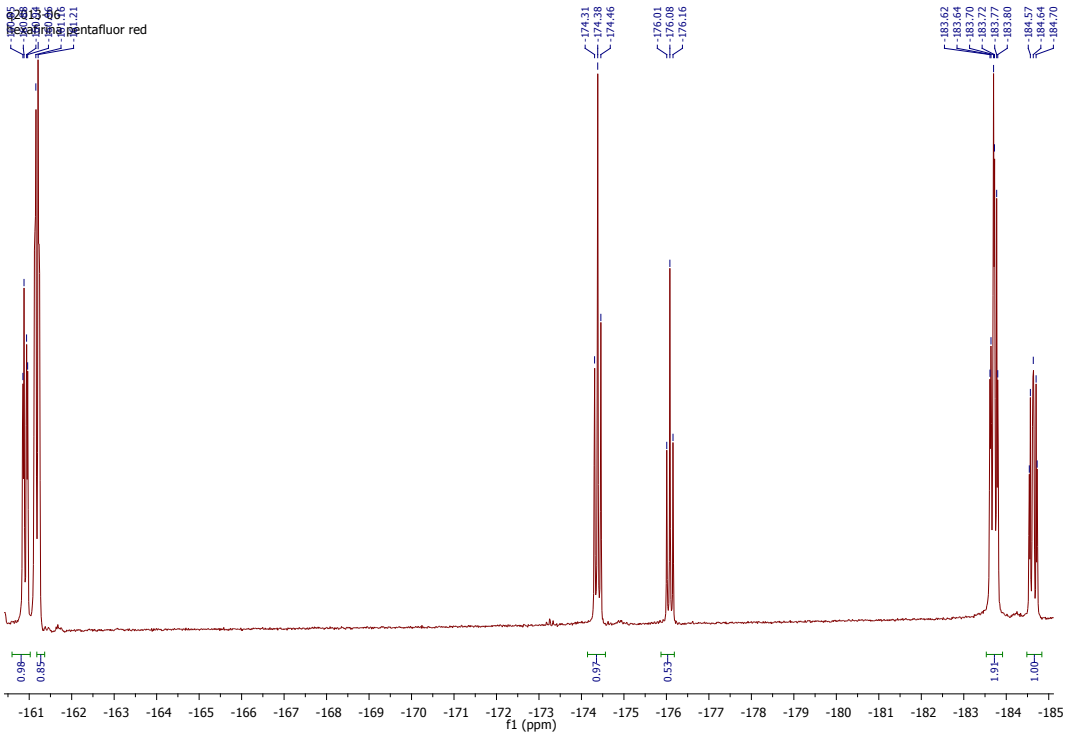

Figure SI 27: ^{19}F NMR spectrum of compound **1** in $CDCl_3$

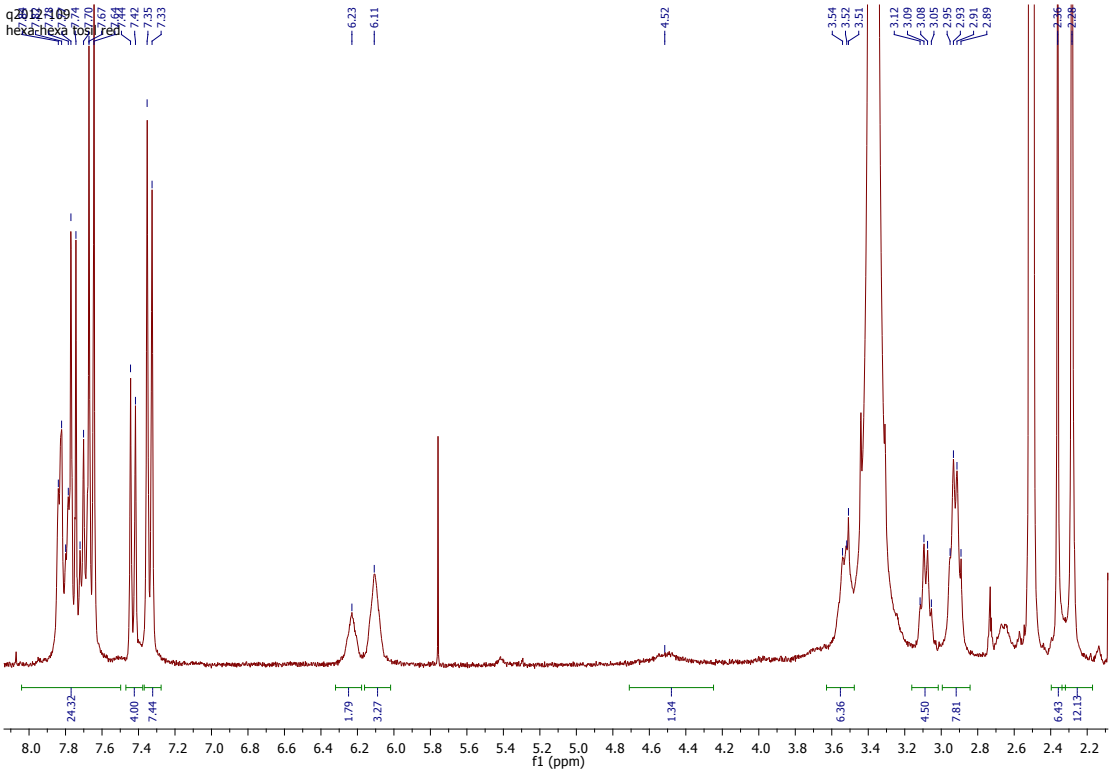

Figure SI 28: ^{1}H NMR spectrum of compound **2** in DMSO-d_6

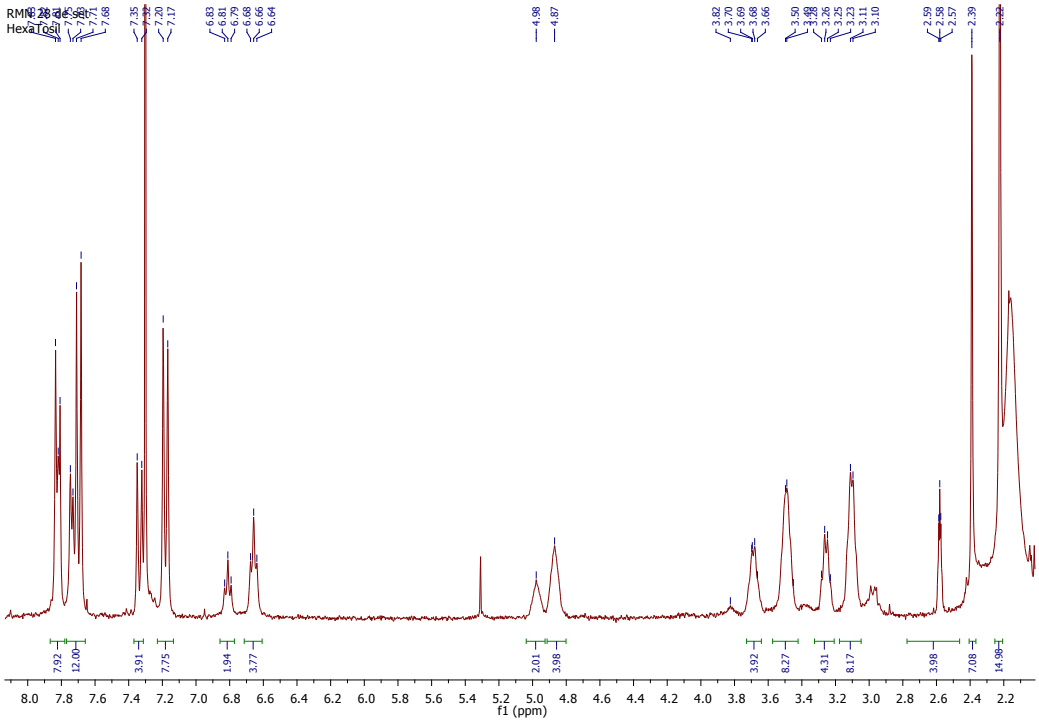

Figure SI 29: ^{1}H NMR spectrum of compound **2** in $CDCl_3$

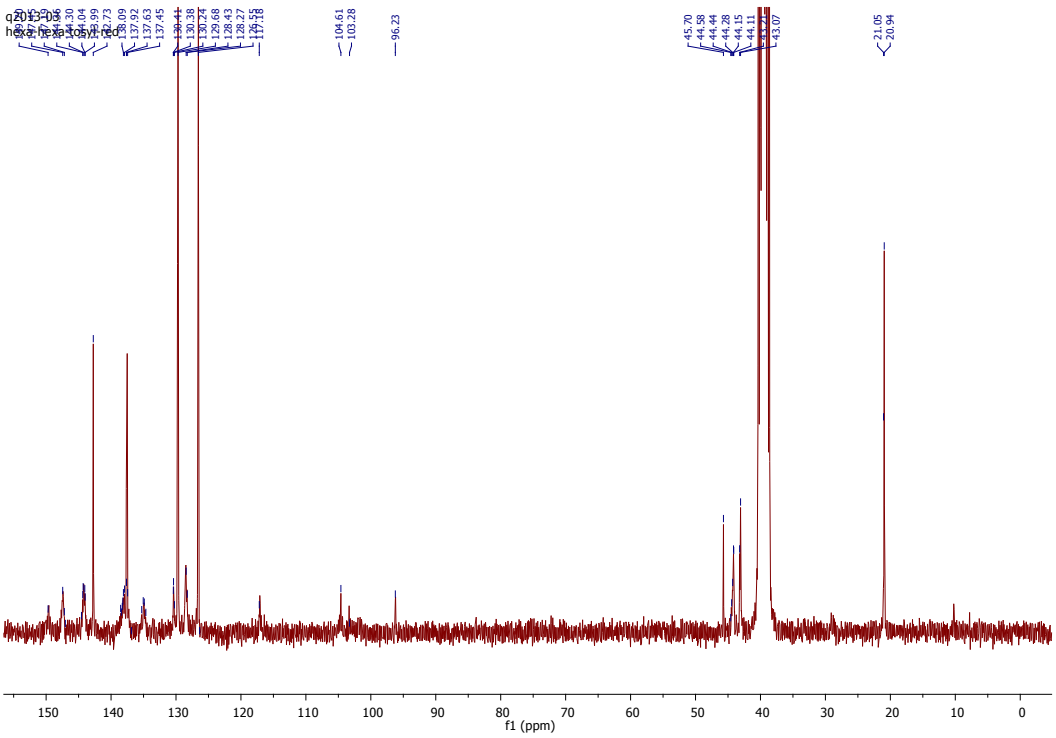

Figure SI 30: ^{13}C NMR spectrum of compound **2** in DMSO-d_6

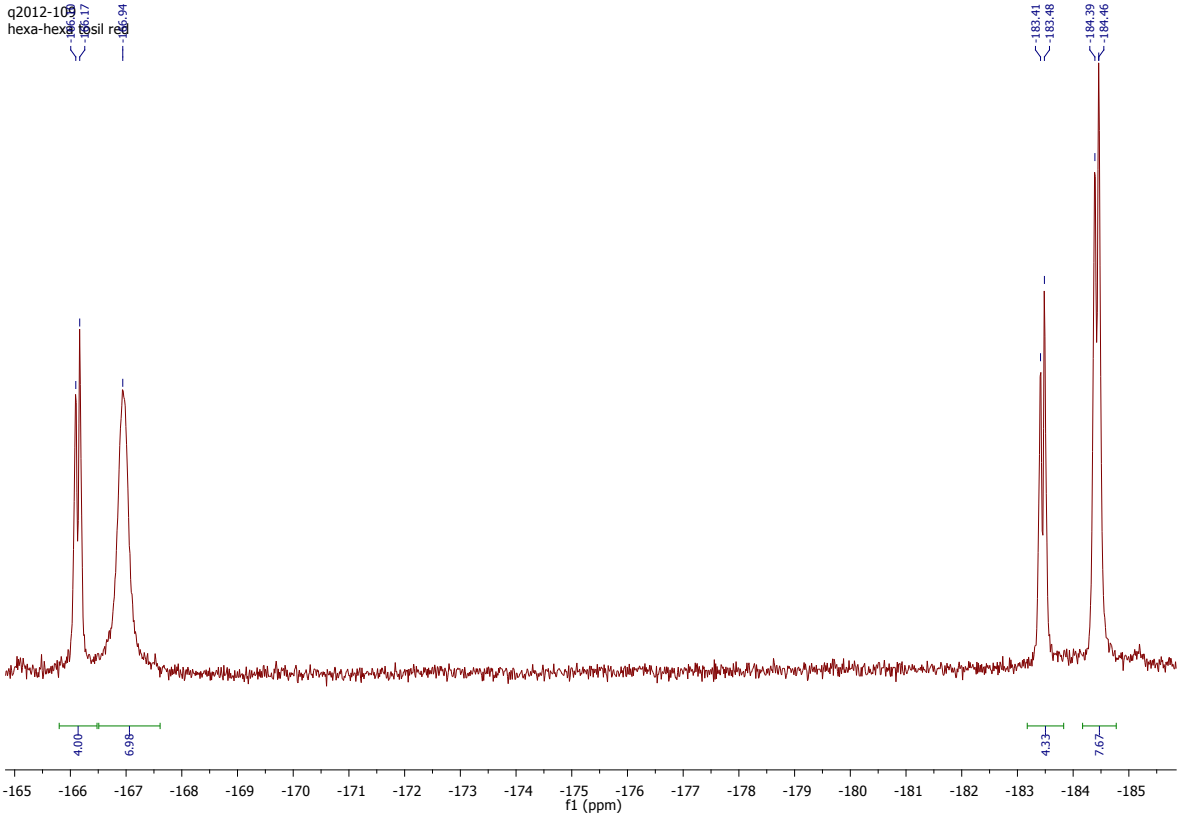

Figure SI 31: ^{19}F NMR spectrum of compound **2** in DMSO-d_6

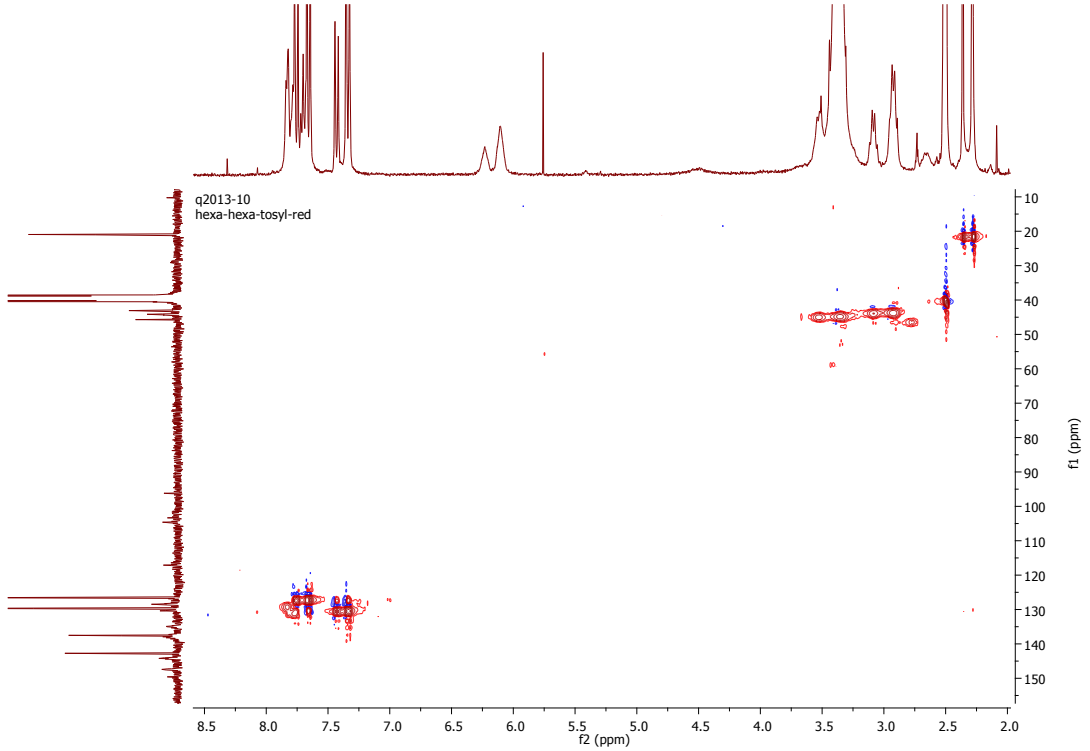

Figure SI 32: HSQC spectrum of compound **2** in DMSO-d_6

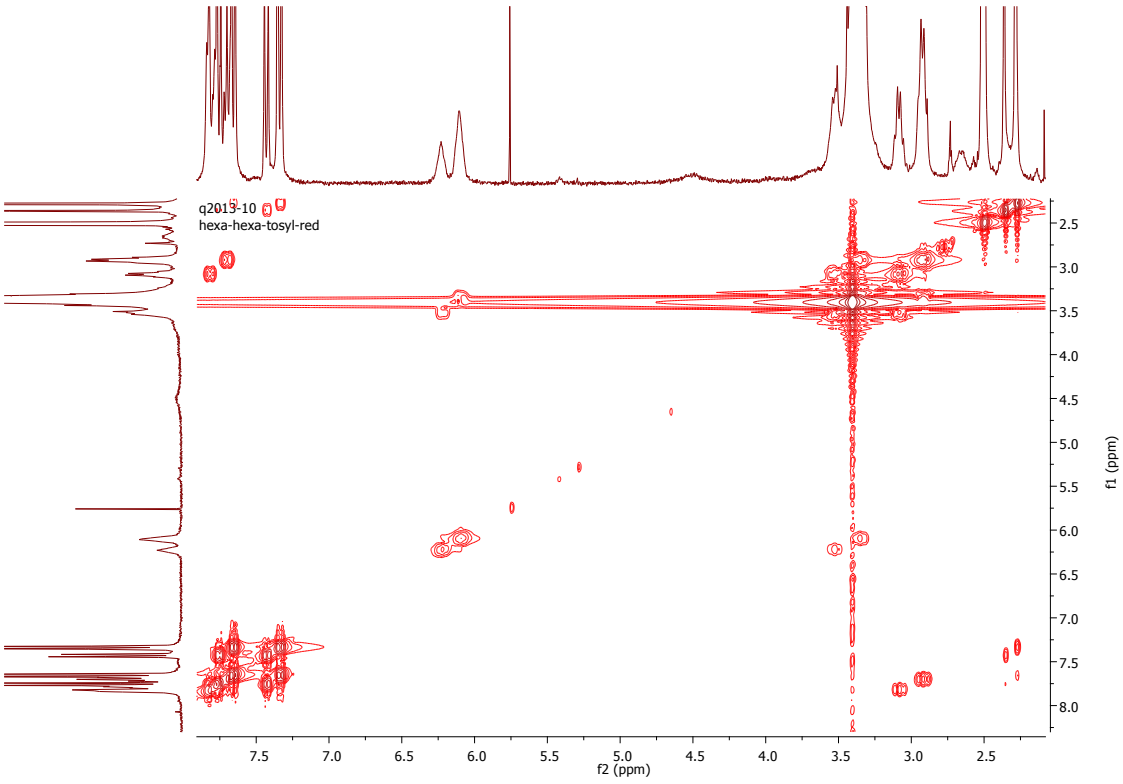

Figure SI 33: COSY spectrum of compound **2** in DMSO-d_6

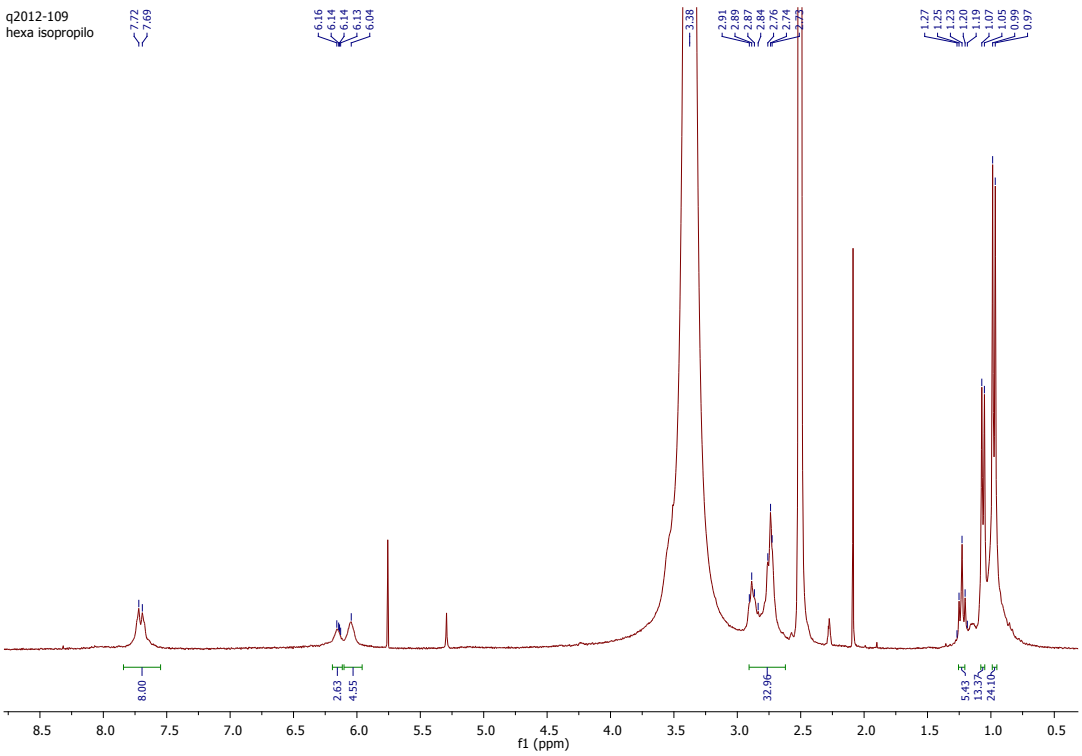

Figure SI 34: ^{1}H NMR spectrum of compound **3** in DMSO-d_6

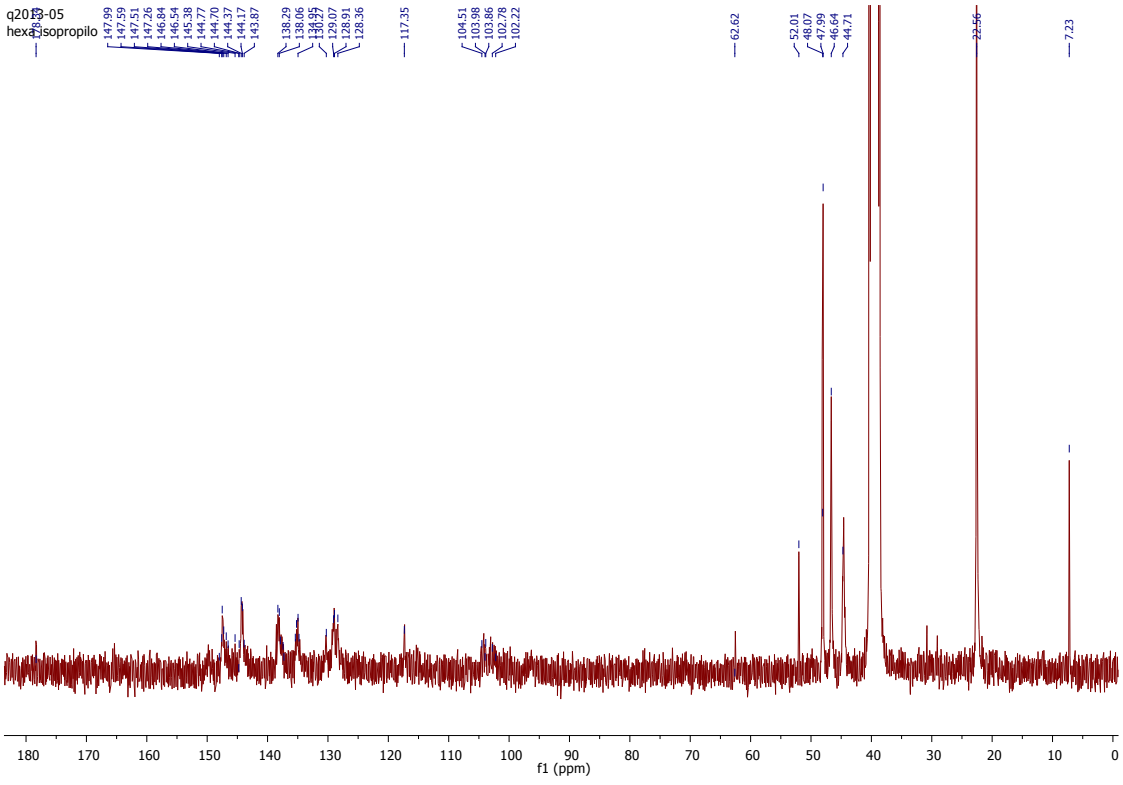

Figure SI 35: ^{13}C NMR spectrum of compound **3** in DMSO-d_6

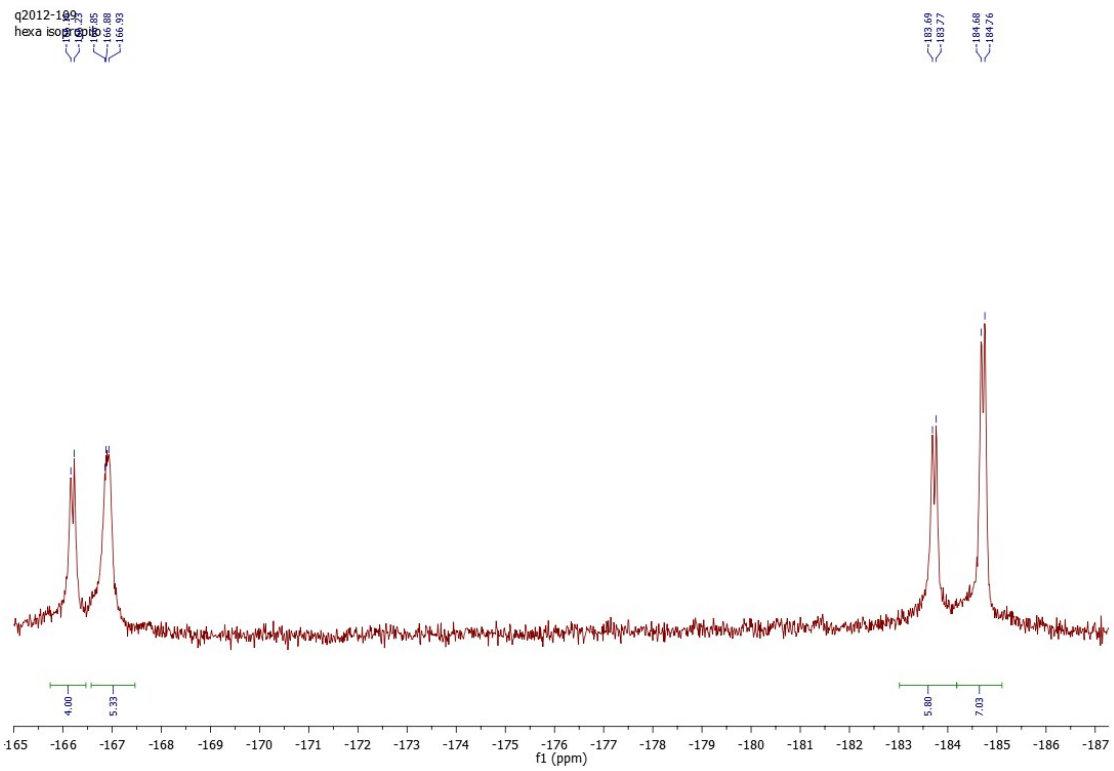

Figure SI 36: ^{19}F NMR spectrum of compound **3** in DMSO-d_6

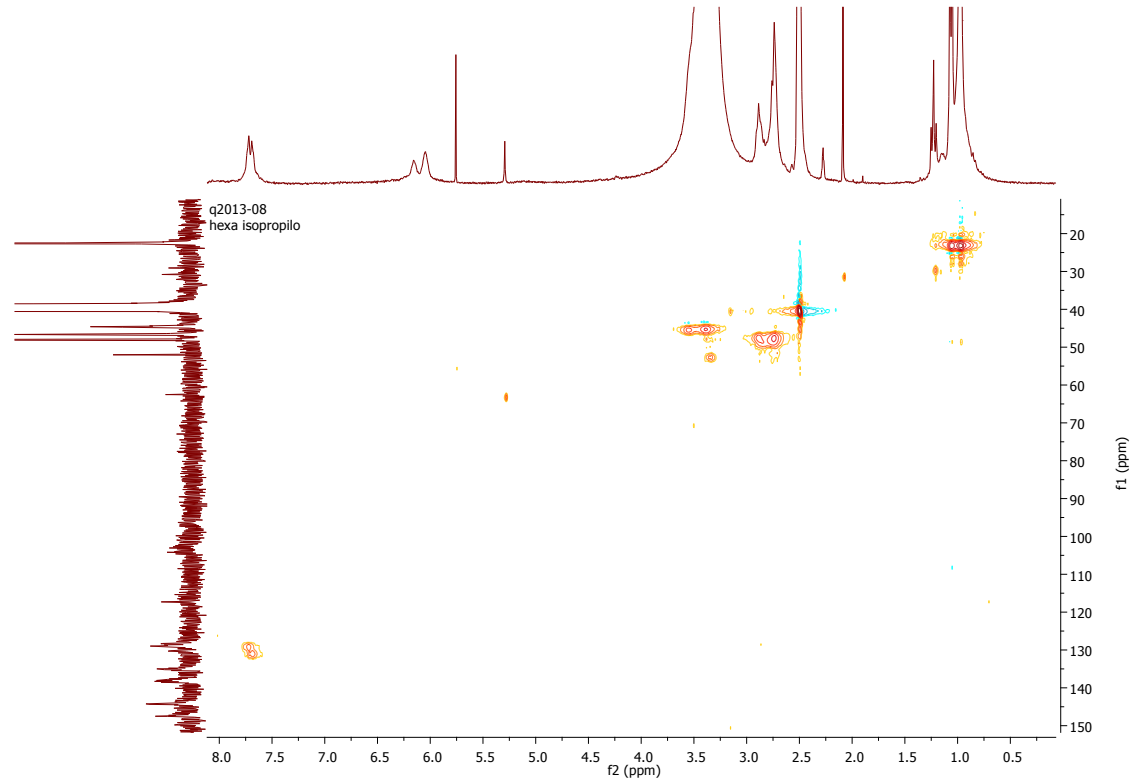

Figure SI 37: HSQC spectrum of compound **3** in DMSO-d_6

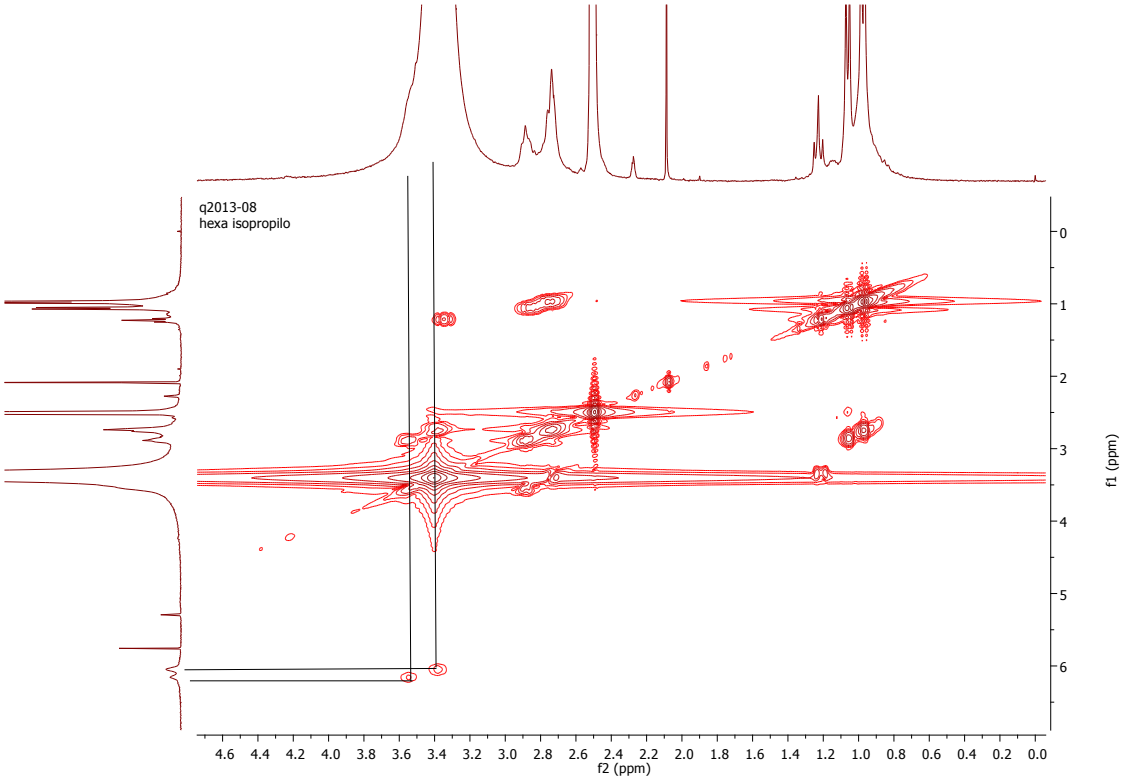

Figure SI 38: COSY spectrum of compound **3** in DMSO-d_6.

Mass Spectrum Molecular Formula Report

Meas. m/z	#	Formula	Score	m/z	err [mDa]	err [ppm]	mSigma	rdb	e⁻ Conf	N-Rule
2625.52241	1	C 121 H 95 F 24 N 17 O 12 S 6	100.00	2625.52816	5.75	2.19	304.0	71.0	odd	ok
	2	C 120 H 93 F 24 N 18 O 12 S 6	12.44	2625.51559	-6.82	-2.60	306.0	71.5	even	ok
2627.53352	1	C 120 H 95 F 24 N 18 O 12 S 6	100.00	2627.53124	-2.28	-0.87	282.1	70.5	even	ok
	2	C 120 H 94 F 24 N 18 O 12 S 6	0.00	2626.52341	-7.15	-2.72	555.6	71.0	odd	ok
	3	C 121 H 93 F 24 N 18 O 11 S 6	0.00	2621.52067	-7.50	-2.85	557.1	72.5	even	ok
	4	C 121 H 94 F 24 N 18 O 11 S 6	0.00	2622.52850	0.12	0.05	557.1	72.0	odd	ok
	5	C 121 H 95 F 24 N 18 O 11 S 6	0.00	2623.53632	7.67	2.92	557.1	71.5	even	ok
	6	C 121 H 94 F 24 N 17 O 12 S 6	0.00	2624.52034	-8.67	-3.30	557.2	71.5	even	ok
	7	C 121 H 95 F 24 N 17 O 12 S 6	0.00	2625.52816	-1.53	-0.58	557.3	71.0	odd	ok
	8	C 121 H 96 F 24 N 17 O 12 S 6	0.00	2626.53599	5.44	2.07	557.3	70.5	even	ok
	9	C 121 H 95 F 23 N 18 O 12 S 6	0.00	2620.53283	4.90	1.86	558.0	72.0	odd	ok
	10	C 121 H 96 F 23 N 18 O 12 S 6	0.00	2621.54066	12.54	4.77	558.0	71.5	even	ok

Figure SI 39: Mass spectrum molecular formula report of compound **2**.

Mass Spectrum Molecular Formula Report

Meas. m/z	#	Formula	Score	m/z	err [mDa]	err [ppm]	mSigma	rdb	e⁻ Conf	N-Rule
1953.74614	1	C 98 H 93 F 22 N 19	58.41	1953.75046	4.31	2.21	481.4	51.0	odd	ok
	2	C 96 H 93 F 24 N 18	100.00	1953.74419	-1.96	-1.00	490.6	47.5	even	ok
1955.75844	1	C 96 H 95 F 24 N 18	100.00	1955.75984	1.40	0.72	130.0	46.5	even	ok
	2	C 98 H 95 F 22 N 19	0.02	1955.76611	7.67	3.92	137.8	50.0	odd	ok

Figure SI 40: Mass spectrum molecular formula report of compound **3**.

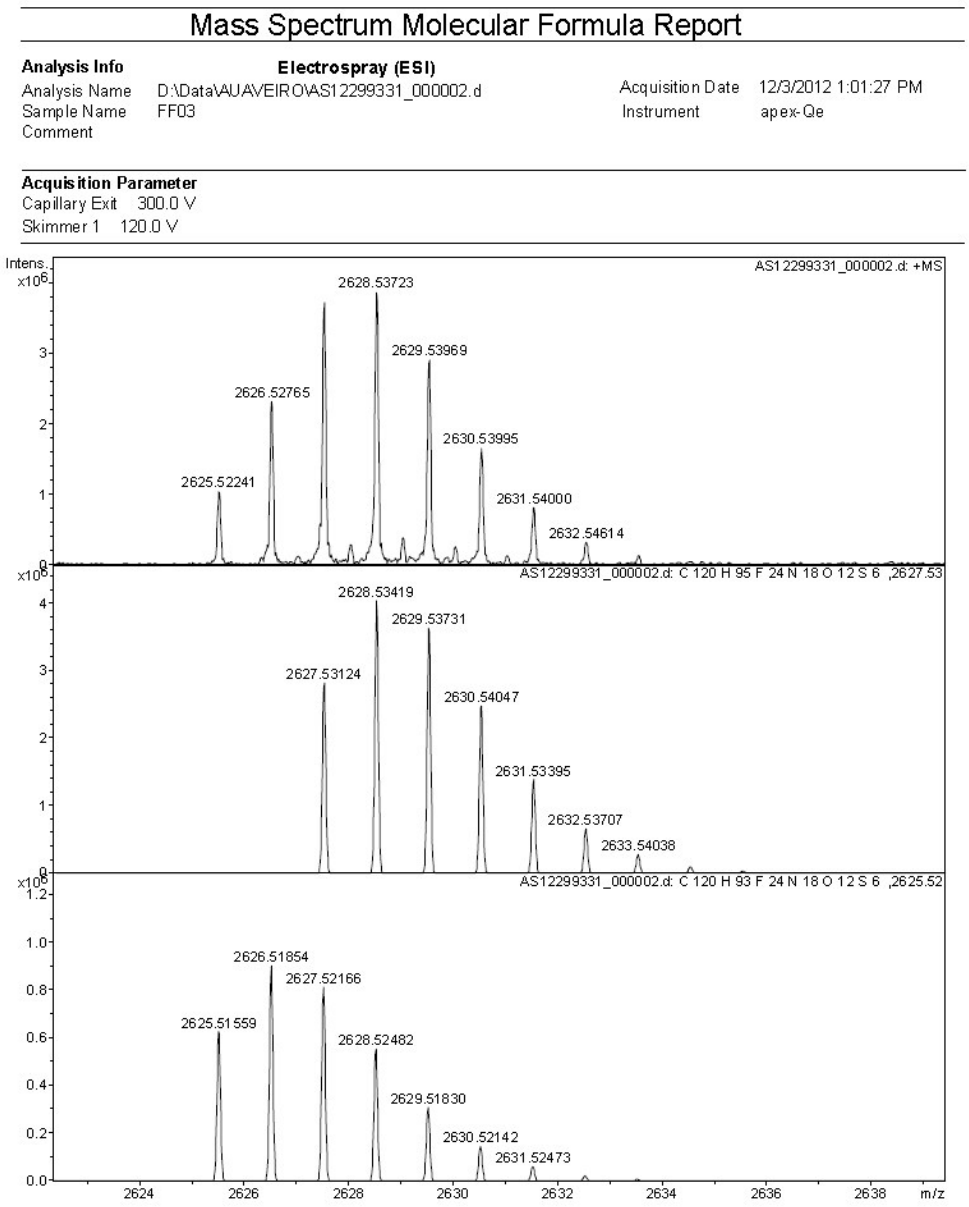

Figure SI 41: Compound **2** molecular envelop compared with their calculated isotopic patterns.

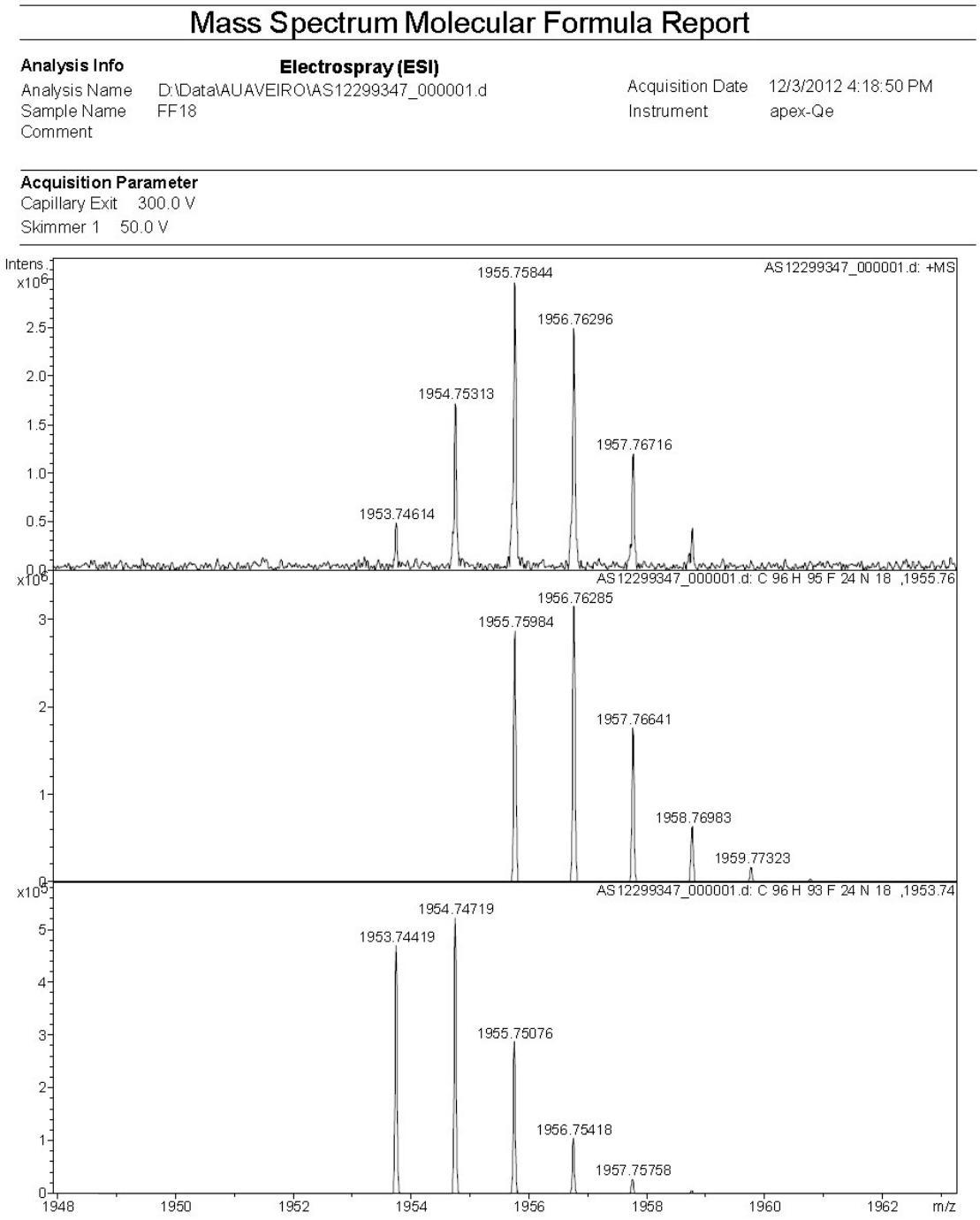

Figure SI 42: Compound **2** molecular envelop compared with their calculated isotopic patterns.

References

1 Shin, J. Y.; Furuta, H.; Yoza, K.; Igarashi, S.; Osuka, A., *J. Am. Chem. Soc*. **2001**, 123 (29), 7190-7191.

2 Connors, K. A. Binding Constants, The Measurement of Molecular Complex Stability; Wiley & Sons: New York, NY, 1987.